New Phytologist

Research

The protein phosphatase subunit PP2A-B′γ is required to suppress day length-dependent pathogenesis responses triggered by intracellular oxidative stress

Shengchun Li[1], Amna Mhamdi[1], Andrea Trotta[2], Saijaliisa Kangasjärvi[2] and Graham Noctor[1]

[1]Institut de Biologie des Plantes, UMR8618 CNRS, Université de Paris sud, 91405 Orsay Cedex, France; [2]Department of Biochemistry, University of Turku, FI-20014 Turku, Finland

Author for correspondence:
Graham Noctor
Tel: +33 169153301
Email: graham.noctor@u-psud.fr

Received: *24 June 2013*
Accepted: *3 November 2013*

New Phytologist (2014) **202:** 145–160
doi: 10.1111/nph.12622

Key words: catalase, hydrogen peroxide (H_2O_2), nitrogen metabolism, PP2A, proteomics, redox, salicylic acid.

Summary

- Oxidative stress responses are influenced by growth day length, but little is known about how this occurs. A combined reverse genetics, metabolomics and proteomics approach was used to address this question in *Arabidopsis thaliana*.
- A catalase-deficient mutant (*cat2*), in which intracellular oxidative stress drives pathogenesis-related responses in a day length-dependent manner, was crossed with a knockdown mutant for a specific type 2A protein phosphatase subunit (*pp2a-b′γ*). In long days (LD), the *pp2a-b′γ* mutation reinforced *cat2*-triggered pathogenesis responses.
- In short days (SD), conditions in which pathogenesis-related responses were not activated in *cat2*, the additional presence of the *pp2a-b′γ* mutation allowed lesion formation, *PATHOGENESIS-RELATED GENE1* (*PR1*) induction, salicylic acid (SA) and phytoalexin accumulation and the establishment of metabolite profiles that were otherwise observed in *cat2* only in LD. Lesion formation in *cat2 pp2a-b′γ* in SD was genetically dependent on SA synthesis, and was associated with decreased *PHYTOCHROME A* transcripts. Phosphoproteomic analyses revealed that several potential protein targets accumulated in the double mutant, including recognized players in pathogenesis and key enzymes of primary metabolism.
- We conclude that the *cat2* and *pp2a-b′γ* mutations interact synergistically, and that PP2A-B′γ is an important player in controlling day length-dependent responses to intracellular oxidative stress, possibly through phytochrome-linked pathways.

Introduction

Modifications of the cellular redox state associated with oxidative stress are an integral part of plant responses to the environment (Apel & Hirt, 2004; Van Breusegem *et al.*, 2008; Foyer & Noctor, 2009). Although increased availability of reactive oxygen species (ROS) can induce malfunction through oxidative modification of sensitive cell components, the phenotypic and physiological outcomes of oxidative stress are mediated by close interactions with signaling through phytohormones, such as salicylic acid (SA), jasmonic acid and ethylene (Overmyer *et al.*, 2003). Because photosynthetic processes, such as chloroplastic electron transport and photorespiration, can be major sources of ROS, the intensity of oxidative stress may be modified by light intensity (irradiance). In addition, growth day length is emerging as a key factor that may modulate ROS availability or, downstream of ROS accumulation, the response to oxidative stress (Bechtold *et al.*, 2005; Becker *et al.*, 2006; Queval *et al.*, 2007, 2012; Vollsnes *et al.*, 2009; Michelet & Krieger-Liszkay, 2011; Kangasjärvi *et al.*, 2012; Dghim *et al.*, 2013; Pérez-Pérez *et al.*, 2013). Because of the centrality of oxidative stress in plant responses to external challenges, an understanding of the underlying factors is potentially relevant to efforts to predict and manipulate stress resistance in the natural environment, where day length is a crucial modulator of plant growth and development.

The Arabidopsis mutant *cat2*, which lacks the major leaf catalase, is a useful study system for the identification of factors involved in the response to hydrogen peroxide (H_2O_2) produced inside the cell through a physiologically relevant pathway (Mhamdi *et al.*, 2010a). Because *CAT2* function is closely linked to photorespiration, loss of its function triggers oxidative stress in plants grown under moderate irradiance in air, when glycolate-dependent H_2O_2 production in the peroxisomes is significant. When grown in these conditions in long days (LD), *cat2* shows decreased growth accompanied by many of the features shown by lesion mimic mutants. This includes many pathogenesis-related (PR) responses, including lesion formation, accumulation of SA and phytoalexins, expression of *PR* genes and induced resistance to bacterial challenge (Chaouch *et al.*, 2010). All of these effects, apart from decreased growth, are annulled in *cat2 sid2* double mutants, in which SA production through the isochorismate pathway is blocked (Chaouch *et al.*, 2010). Similar decreases in

growth in *cat2 sid2* and *cat2*, as well as the responses of biochemical and transcriptomic markers of the redox state, show that *cat2*-triggered intracellular oxidative stress and SA-dependent responses can be uncoupled.

Responses to oxidative stress in *cat2* are strongly influenced by day length. When the mutant is grown under moderate or even high light in short days (SD), oxidative stress is apparent, but lesions are absent and SA-dependent responses are not activated (Queval *et al.*, 2007; Chaouch *et al.*, 2010). Moreover, distinct transcriptomic and metabolomic signatures are observed in *cat2* grown in SD or LD conditions (Queval *et al.*, 2007, 2012; Chaouch *et al.*, 2010). The conditional day length-dependent nature of the oxidative stress responses in *cat2* implies that genetic factors interact with the environment to govern responses to oxidative stress.

Genetic factors determine cell death triggered by excess singlet oxygen generation in the *fluorescent* (*flu*) mutant (Wagner *et al.*, 2004). The SA-dependent lesion phenotype observed in *cat2* in LD is also strongly modulated by secondary mutations, including several that cause loss of function of recognized players in pathogenesis pathways, such as *NONEXPRESSOR OF PATHOGENESIS-RELATED GENES1* (*NPR1*) and *Arabidopsis thaliana respiratory burst oxidase homolog F* (*AtRbohF*) (Chaouch *et al.*, 2010, 2012; Han *et al.*, 2013a,b). It is also affected by genetically blocking glutathione accumulation and by mutations in certain NADPH-producing enzymes (Mhamdi *et al.*, 2010b; Han *et al.*, 2013a,b). Despite the clear effect of these secondary mutations on *cat2* responses in LD, we have identified none that permit oxidative stress to trigger lesions and related responses in *cat2* grown in SD conditions. The factors that repress oxidative stress-triggered pathogenesis responses in SD conditions therefore remain unknown.

Although much remains to be elucidated on the link between oxidative stress and pathogenesis responses, protein phosphorylation status is involved (Kovtun *et al.*, 2000; Apel & Hirt, 2004). Type 2A protein phosphatases (PP2A) account for a significant part of total protein phosphatase activity in plant tissue extracts (MacKintosh & Cohen, 1989). These enzymes are composed of three types of subunit (A, B, C), with each subunit being encoded by several genes. Theoretically, the interaction of A, B and C subunits encoded by the different genes could produce 255 possible heterotrimeric combinations, allowing a potentially wide range of specific functions in protein dephosphorylation (Zhou *et al.*, 2004). Genes encoding the regulatory B subunit are the most numerous (17 genes, subclassified into B, B′ and B″), probably reflecting the importance of these polypeptides in determining the substrate specificities and physiological functions of the different PP2A holoenzymes. Recently, novel roles for a gene encoding a specific PP2A-B′ subunit have been described (Trotta *et al.*, 2011a, b). Loss-of-function mutants for PP2A-B′γ were shown to constitutively activate pathogenesis responses (Trotta *et al.*, 2011a). However, how this PP2A subunit functionally interacts with ROS and the cellular redox state remains unknown. Outstanding questions include: (1) whether PP2A-B′γ interacts with day length to influence oxidative stress outcomes; (2) the proteins that may be affected by PP2A-B′γ during any such function; (3) the influence of PP2A-B′γ in oxidative stress-triggered modulation of plant metabolism; and (4) whether this subunit plays a role in signaling upstream or downstream of intracellular oxidative stress.

Through a genetics-based analysis of the interaction between intracellular oxidative stress and PP2A-B′γ, this study provides new information on these questions. Most notably, we show that the repression of SA-dependent PR responses when oxidative stress is occurring in SD is dependent on PP2A-B′γ, and report novel proteomics data on PP2A-B′γ-sensitive phosphorylation targets during intracellular oxidative stress.

Materials and Methods

Plant material

The species studied was *Arabidopsis thaliana* (L.) Heynh T-DNA, and other mutant lines were all generated in the Col-0 background. The *cat2* line was *cat2-1* (Queval *et al.*, 2009) and the *pp2a-b′γ* mutant was SALK_039172 (Trotta *et al.*, 2011a). The *cat2 pp2a-b′γ* line was produced by crossing, and triple mutants were obtained by crossing the double mutant with *cat2 sid2* or *cat2 npr1*, lines that have been described previously (Chaouch *et al.*, 2010; Han *et al.*, 2013a).

Identification of homozygous double and triple mutants

After verification of double heterozygotes in the F1 generation by PCR, double and triple homozygotes were identified similarly in plants grown from F2 seeds. For T-DNA insertions, leaf DNA was amplified by PCR (30 s at 94°C, 30 s at 60°C, 1 min at 72°C, 30 cycles) using primers specific for left T-DNA borders and the *CAT2* and *PP2A-B′γ* genes (Supporting Information Table S1). Zygosity of the *SA induction-deficient 2* (*sid2*) and *npr1* mutations was established using restriction length polymorphism (Fig. S1). Functional analyses were performed on plants grown from F3 seeds.

Plant growth and sampling

Unless indicated otherwise, plants were grown in a controlled environment growth room under a day : night regime of 8 h : 16 h (SD) or 16 h : 8 h (LD), an irradiance of 200 μmol m^{-2} s^{-1} at leaf level, temperatures of 20°C day : 18°C night, 65% humidity and a CO_2 concentration of 400 μl l^{-1}. Nutrient solution was supplied twice per week. Plants were analyzed and sampled at the age of 21–24 d (LD) and 35 d (SD). For complementation experiments, plants were grown in SD for 5 wk, and 10 mM myo-inositol was sprayed onto the rosettes daily from the fourth week onwards. Samples were taken in the middle of the photoperiod ($n = 3$–5 independent biological replicates), rapidly frozen in liquid nitrogen and stored at −80°C. The percentage lesion areas on the leaves were quantified using IQmaterials software. Significant differences are expressed using Student's *t*-test at $P < 0.05$. All experiments were repeated at least

twice with similar results. Staining with 3,3′-diaminobenzidine (DAB) was performed as in Mhamdi *et al.* (2010c).

Quantitative PCR (qPCR) analysis

RNA was extracted using the TRIZOL reagent (Life Technologies, Saint Aubin, France). cDNA was produced by reverse transcription using the SuperScript™ III First-Strand Synthesis System (Invitrogen, Carlsbad, CA, USA). qPCR was performed as in Queval *et al.* (2007). Primer sequences are listed in Table S1.

Metabolite profiling

Targeted analysis of antioxidants was performed by plate-reader (Queval & Noctor, 2007). SA, scopoletin and camalexin were measured by high-performance liquid chromatography (HPLC)-fluorescence as in Langlois-Meurinne *et al.* (2005). Non-targeted metabolite profiling by gas chromatography-time of flight-mass spectrometry (GC-TOF-MS) followed previously described protocols (Noctor *et al.*, 2007; Chaouch *et al.*, 2012). Details are provided in Table S2(c). Peak deconvolution and integration of specific ions were performed using the LECO Pegasus software, based on mass spectra available in the National Institute of Standards and Technology (NIST) and MPI-GOLM reference libraries, as well as an in-house database generated using authentic standards. To produce the heatmap display, values were centered and reduced. For each compound, means and standard deviations were calculated across all samples. For each genotype, the mean value for compound '*x*' was subtracted from the mean across all samples, and the value was then divided by the overall standard deviation for that compound.

Proteomics

Extraction of total foliar extracts and total soluble leaf extracts was performed in the presence of protease (Complete-Mini; Roche) and phosphatase (PhosSTOP; Roche) inhibitors using the methods described by Kangasjärvi *et al.* (2008). Total soluble leaf extracts and membrane fractions corresponding to 80 μg of proteins were used for mono-dimensional sodium dodecylsulfate-polyacrylamide gel electrophoresis (SDS-PAGE) or CN-PAGE (clear-native PAGE) followed by SDS-PAGE. Soluble oligomeric protein complexes were separated by CN-PAGE followed by SDS-PAGE in the second dimension according to Peltier *et al.* (2006) with the modifications for buffers described by Rokka *et al.* (2005), except that only 0.05% deoxycholate was used as a detergent on CN gels. After imaging the gels with Sypro Ruby (Invitrogen), MS was performed as described by Peltier *et al.* (2006) using a liquid chromatography-electrospray ionization-MS/MS system (Q-Exactive; Thermo Fisher Scientific, Waltham, MA, USA, and QTOF Elite; AB Sciex, Framingham, MA, USA). MS/MS spectra were analyzed with an in-house installation of Mascot (www.matrixscience.com), with searches restricted to the Uniprot Arabidopsis database. Results were analyzed through Proteome Discover v.1.3 (Thermo Scientific) allowing methionine (Met) oxidation, cysteine (Cys) carboamidomethylation and serine/threonine (Ser/Thr) and tyrosine (Tyr) phosphorylation as possible modifications, and validating the phosphopeptides through PhosphoRS filter and Decoy Database Search, with target false discovery rates (FDR) of < 0.01 (strict) and < 0.05 (relaxed). The confidence threshold for phosphopeptides was set to $P < 0.05$. Phosphopeptides above this threshold were validated manually.

Results

The *pp2a-b′γ* mutant has been characterized and described previously by Trotta *et al.* (2011a). To explore interactions between intracellular oxidative stress and PP2A-B′γ function, this line was crossed with *cat2* to produce double mutants, and the interplay between the two mutations in determining phenotypes, defense and metabolic responses was examined in LD (16 h photoperiod) and SD (8 h photoperiod) conditions.

Interactions between *cat2* and *pp2a-b′γ* mutations during growth in LD

First, plants were analyzed by following growth in LD at moderate light, conditions in which pathogenesis responses are activated by oxidative stress in *cat2*. All three mutant lines were smaller than the wild-type, with the double mutant showing a significant decrease relative to *cat2* (Fig. 1a). Lesions were clearly apparent in both *cat2* backgrounds, and slightly more extensive in *cat2 pp2a-b′γ*. The *pp2a-b′γ* single mutant also presented some lesions, although to a much lesser extent than *cat2* (Fig. 1a). There was an overall correlation between lesion extent and expression of *PATHOGENESIS-RELATED GENE1* (*PR1*). This SA marker gene was strongly induced in *cat2*, but not significantly in *pp2a-b′γ* (Fig. 1b). In the double mutant, *PR1* expression was increased to about two-fold the *cat2* values (Fig. 1b). Analysis of SA and related defense compounds showed a similar pattern, with some induction in the *pp2a-b′γ* mutant and stronger induction in *cat2*. The double mutant generally showed the most marked accumulation of these compounds, and this was particularly apparent for camalexin, a major phytoalexin in Arabidopsis (Glawischnig, 2007), which was about three-fold higher in *cat2 pp2a-b′γ* than in *cat2* (Fig. 1c). Together, these observations show that loss of *PP2A-B′γ* function produces the activation of defense responses, as reported previously (Trotta *et al.*, 2011a), and that the mutation reinforces these responses in *cat2*.

In our hands, changes in H_2O_2 are negligible in *cat2*, either because of rapid metabolism by alternative pathways, technical difficulties in the specific quantification of this reactive molecule, or both (Queval *et al.*, 2008; Mhamdi *et al.*, 2010a,c). Increased accumulation of oxidized glutathione is a well-described response in catalase-deficient plants (Smith *et al.*, 1984; Willekens *et al.*, 1997), and is the clearest biochemical marker of oxidative stress in *cat2* (Queval *et al.*, 2007; Mhamdi *et al.*, 2010a,c). This key determinant of intracellular thiol-disulfide status is clearly implicated in pathogenesis and other plant stress responses (Ball *et al.*, 2004; Parisy *et al.*, 2007), and is functionally important in determining the activation of phytohormone signaling and related

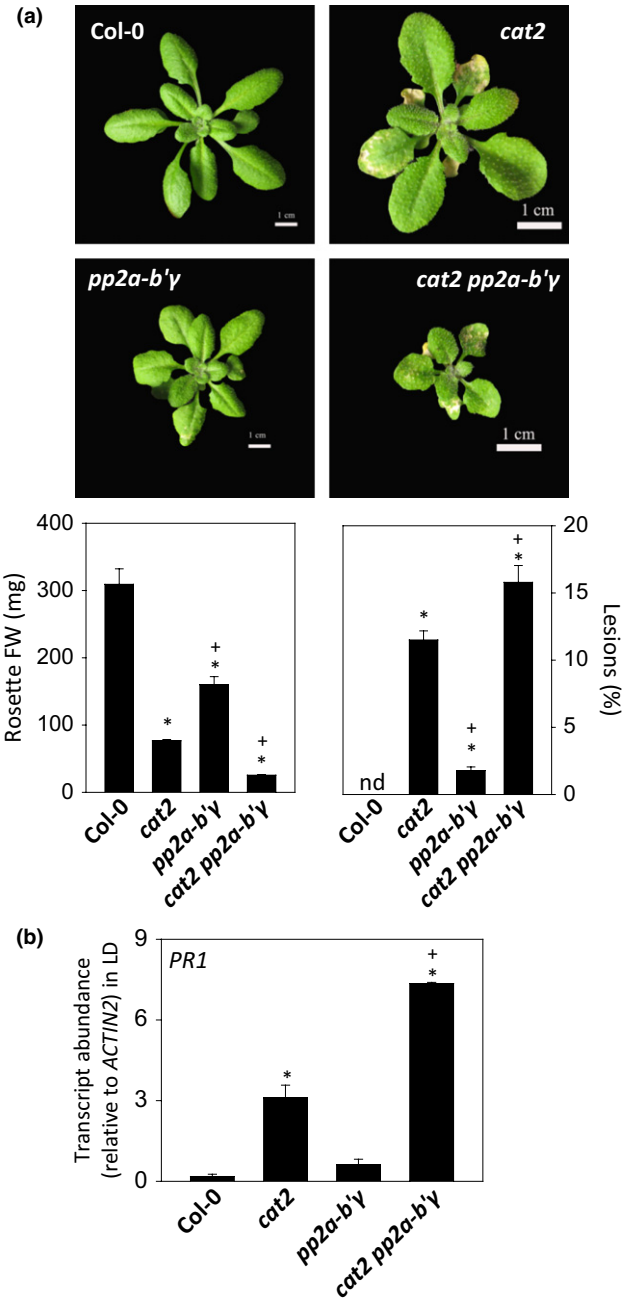

Fig. 1 Growth and pathogenesis-related responses in Arabidopsis Col-0, *cat2*, *pp2a-b'γ* and *cat2 pp2a-b'γ* growing in long days (16 h light : 8 h dark). (a) Representative photographs of plants and quantification of rosette mass and lesion area. (b) *PATHOGENESIS-RELATED GENE1* (*PR1*) expression measured by quantitative PCR (qPCR). (c) Salicylic acid (SA) and related defense compounds. Data are means ± SE of at least 10 plants (a) or three to four biological replicates (b, c). * and +, significant difference relative to Col-0 or to *cat2* ($P < 0.05$). FW, fresh weight; nd, not detected.

phenotypes in *cat2* grown in LD (Han *et al.*, 2013a,b). Like glutathione, ascorbate is a marker of tissue redox status, and has been implicated in responses to biotic stress (Pastori *et al.*, 2003). The reduced and oxidized forms of these two molecules were therefore quantified as markers of cellular redox state.

In all mutants, ascorbate was slightly more oxidized than in Col-0, but, in agreement with previous studies, its status was much less affected than glutathione by the *cat2* mutation (Fig. S2). In *cat2*, glutathione was increased *c.* 2.5-fold, and this was associated with a drop in the redox state from over 90% to *c.* 60% reduced (Fig. S2). Slight oxidation of glutathione was also observed in *pp2a-b'γ*, but the combination of the two mutations did not cause further oxidation or accumulation relative to *cat2* (Fig. S2).

One feature of the *cat2* mutant is its conditional photorespiratory nature. This means that this line shows little sign of oxidative stress when grown at high CO_2 or low light, conditions in which photorespiration is negligible or slow. At low light, the *pp2a-b'γ* mutant showed a similar decrease in growth to that observed at moderate light (Fig. S3). By contrast, the impact of the *cat2* mutation on rosette size or glutathione status was much less marked than at the standard irradiance (compare data in Figs 1 and S3). In low light conditions, no lesions were detectable on the leaves of any of the mutants. Experiments in which plants were grown at high CO_2 also revealed that no lesions were observed on single or double mutants (data not shown). Thus, whether or not *PP2A-B'γ* was functional, lesions triggered by the

cat2 mutation were conditionally dependent on a threshold rate of photorespiratory H_2O_2 production, and the oxidative stress that resulted from it.

Effect of the *pp2a-b′γ* mutation in SD, conditions that are non-permissive for the activation of pathogenesis responses in *cat2*

Because the above data reveal a functional interaction between the *pp2a-b′γ* and *cat2* mutations on the pathogenesis responses in LD, we focused the remainder of our study on establishing whether *PP2A-B′γ* could be involved in regulating these responses in *cat2* grown in SD. When plants were grown in SD at the same irradiance as in LD (Fig. 1), oxidative stress in *cat2* produced a decrease in growth, but no lesions were observed and *PR1* was not induced (Fig. 2). Lesions were also absent on the leaves of *pp2a-b′γ*. By contrast, the *cat2 pp2a-b′γ* double mutant showed significant lesion formation and induction of *PR1* (Fig. 2). Unlike *cat2*, the double mutant also showed significant DAB staining (Fig. 2).

Redox analysis revealed that the appearance of lesions in the double mutant was not associated with marked increases in oxidation of either ascorbate or glutathione relative to *cat2* (Fig. 3). Similar to effects observed in LD (Fig. S2), the double mutant showed a slight tendency to increased oxidation of ascorbate (Fig. 3). The *pp2a-b′γ* mutation did not affect glutathione status in the Col-0 background. In *cat2* in SD, glutathione was even more oxidized than in LD (Fig. 3; compare with data in Fig. S2), but neither the oxidation state nor the accumulation was further increased by the secondary *pp2a-b′γ* mutation. Indeed, the lesions observed in SD in the double mutant (Fig. 2) were associated with a more reduced glutathione pool than in *cat2* (Fig. 3), in which no lesions were apparent in this condition (Fig. 2).

To identify the metabolic changes underlying the lesions induced in *cat2 pp2a-b′γ* in SD, non-targeted profiling of almost 100 metabolites was performed by GC-TOF-MS (Table S2). Using this technique, we have previously identified a specific metabolite signature induced by intracellular oxidative stress in an LD- and SA-dependent manner (Chaouch *et al.*, 2010). This signature shows considerable overlap with that induced by bacterial challenge, and its main features are absent in both *cat2* grown in SD and in a *cat2 sid2* mutant in LD (Chaouch *et al.*, 2010, 2012). Hierarchical clustering of all metabolites quantified in samples taken in SD revealed that the single *cat2* and *pp2a-b′γ* mutations had only a minor impact (Fig. 4, left). By contrast, a marked effect on metabolite profiles was observed in the double mutant (Fig. 4, left). This involved the accumulation of a large subcluster of compounds that accumulated much less or not at all in the *cat2* single mutant. Comparison with a previously described dataset revealed that most of these compounds were those that accumulated in the *cat2* single mutant in LD, but not in *cat2 sid2* (Fig. 4). Thus, the *pp2a-b′γ* mutation allows intracellular oxidative stress to induce metabolic responses in SD that are only observed in LD when *PP2A-B′γ* is functional, and these responses are dependent on the isochorismate pathway of SA

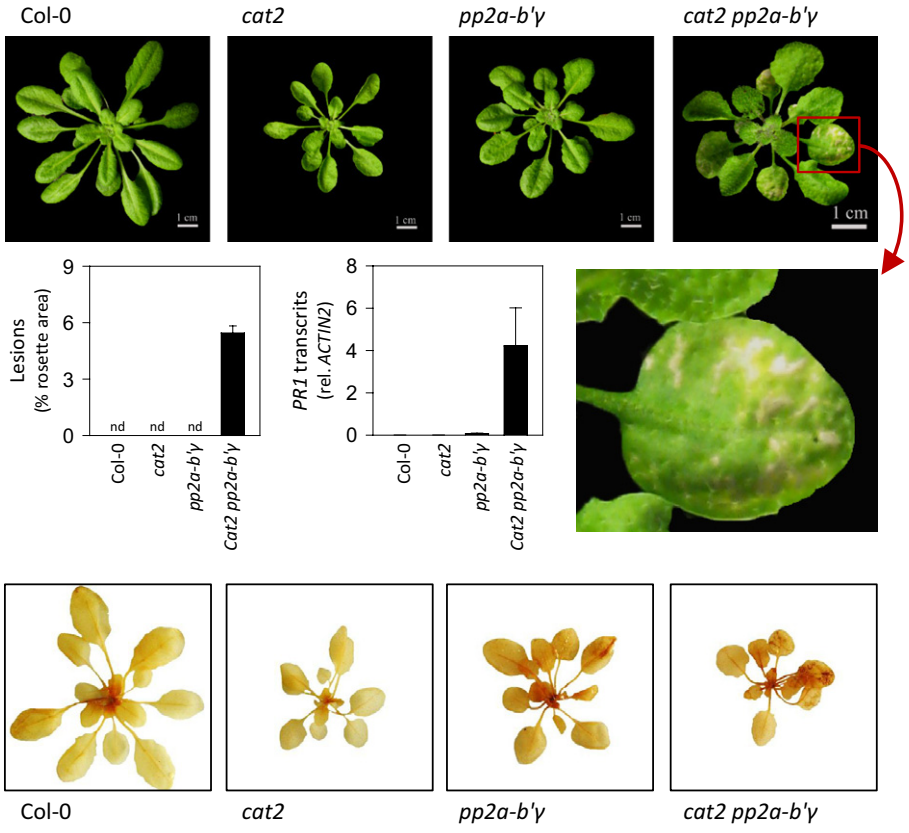

Fig. 2 The *pp2a-b′γ* mutation allows intracellular oxidative stress to trigger lesions and *PATHOGENESIS-RELATED GENE1* (*PR1*) expression responses in Arabidopsis in otherwise non-permissive conditions (short days; 8 h light : 16 h dark). Data are means ± SE of at least 10 plants (lesions) or five biological replicates (*PR1*). Photographs at the bottom show staining of tissues with 3,3′-diaminobenzidine (DAB). Note that the top and bottom series of photographs show different plants; nd, not detected.

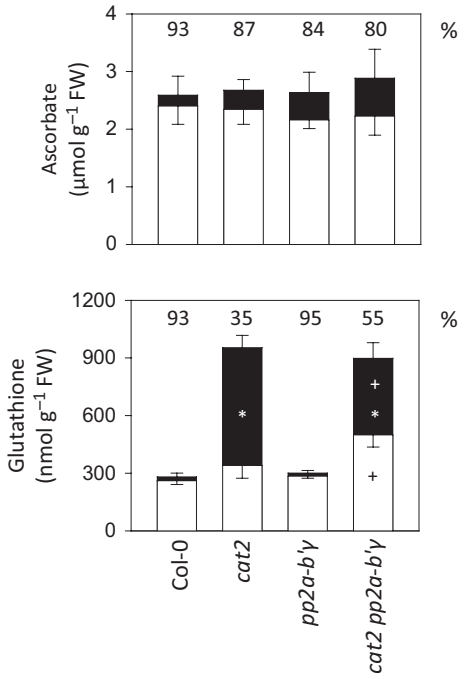

Fig. 3 Major leaf antioxidant pools in Arabidopsis Col-0, *cat2*, *pp2a-b′γ* and *cat2 pp2a-b′γ* growing in short days. White bars, reduced forms; black bars, oxidized forms. Data are means ± SE of three biological replicates. Where significant, * and + indicate difference relative to Col-0 or to *cat2* ($P < 0.05$) for each form. Numbers above the bars indicate the percentage of ascorbate or glutathione in the reduced form. FW, fresh weight.

synthesis. Indeed, SA itself was among the metabolites that were most clearly dependent on the *cat2–pp2a-b′γ* interaction (Fig. 4). Others included nicotinic acid, which has been implicated in pathogenesis responses (Noctor *et al.*, 2011), and gluconic acid, which is strongly induced by bacterial challenge as well as in *cat2* in LD (Chaouch *et al.*, 2012; Tables 1, S2).

The combined presence of the two mutations produced striking changes in many amino acids. In our conditions, although minor increases in homoserine and tryptophan were apparent, the *pp2a-b′γ* single mutant showed amino acid profiles that were similar to those of the wild-type (Fig. S4). When introduced into the *cat2* background, the *pp2a-b′γ* mutation markedly stimulated amino acid accumulation. In some cases, the main effect was to reinforce increases that were already evident in *cat2* (e.g. glutamate, glutamine, Cys, Met, Ser, *O*-acetylserine). In many cases, however, the two mutations acted together to produce increases that were minor or negligible in the single mutants. Striking examples of compounds that responded in this way were isoleucine, ornithine, Thr, lysine, β-alanine, GABA, phenylalanine, Tyr, tryptophan and arginine (Fig. S4), the last two featuring among the most strongly induced significant metabolites observed in *cat2 pp2a-b′γ* (Table 1).

To further investigate the role of SA, this compound was quantified by HPLC in plants grown in SD, together with the phytoalexin, camalexin. Despite the evident disulfide stress in *cat2* (Fig. 3), the amounts of SA and camalexin were not significantly different from those in Col-0 (Fig. 5). Some induction of

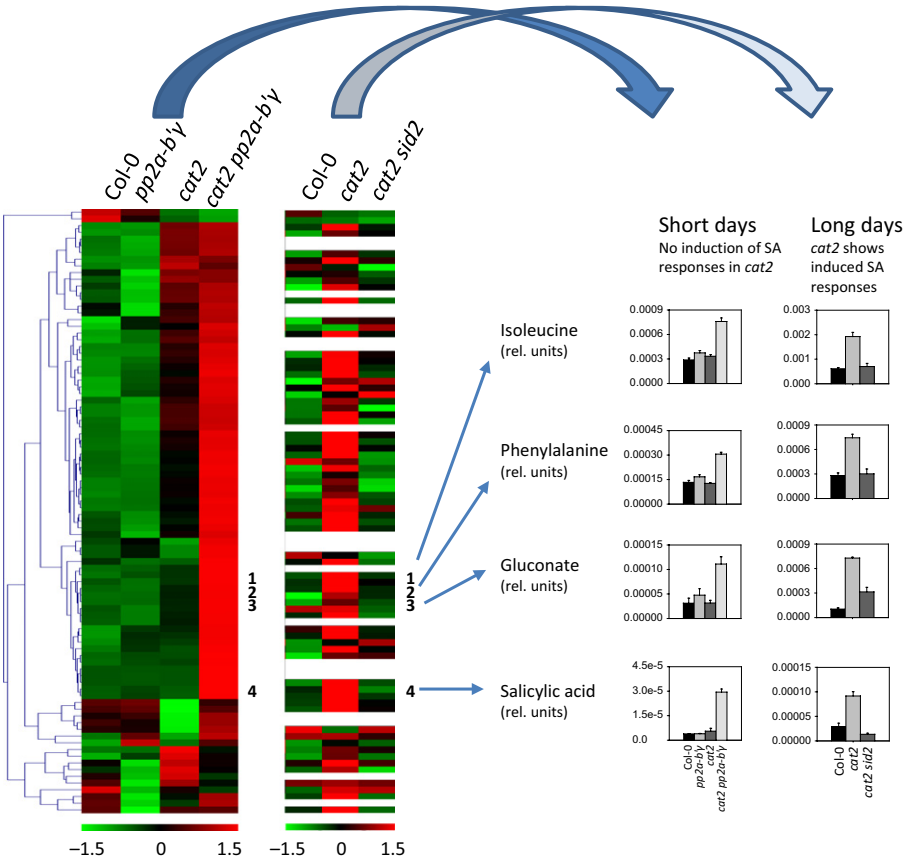

Fig. 4 Gas chromatography-time of flight-mass spectrometry (GC-TOF-MS) analysis of Arabidopsis leaves reveals that the *pp2a-b′γ* mutation allows the induction of *cat2* metabolite profiles in short days that are only otherwise induced in long days in an ISOCHORISMATE SYNTHASE1 (ICS1)-dependent manner. Left heatmap, display of identified metabolites in the four plant lines grown in short days. Right heatmap, corresponding data from Chaouch *et al.* (2010), replotted in a new form, for Col-0, *cat2* and *cat2 sid2* grown in long days. White rows indicate metabolites that were not detected in at least one sample in the previous analysis. Graphs on the right show selected metabolites that are induced in *cat2 pp2a-b′γ* in short days, with a comparison of their response in *cat2* and *cat2 sid2* in long days (means ± SE of three biological replicates).

Table 1 The most induced metabolites in the leaves of the Arabidopsis *cat2 pp2a-b′γ* double mutant in short days (SD). Fifty-three significantly different metabolites were identified in *cat2 pp2a-b′γ* relative to Col-0 (Table S2b). The 10 most induced of these are shown below

	Fold changes			
	Short days (this study)			Long days (Chaouch *et al.*, 2012)
Metabolite	*cat2* rel. Col-0	*cat2 pp2a-b′γ* rel. Col-0	*cat2 pp2a-b′γ* rel. *cat2*	*cat2* rel. Col-0
Nicotinic acid	1.0	95.1*	94.0*	3.9
Gluconic acid	26.7*	53.9*	2.0*	95.9
Norvaline	13.0*	17.8*	1.4	ND
Aminoadipic acid	1.0	12.2*	12.0*	+
2-Hydroxyglutaric acid	1.0	10.8*	10.6*	13.6
Arginine	1.7	10.5*	6.1*	5.4
Tryptophan	1.0	9.15*	9.0*	+
Salicylic acid	1.0	7.6*	7.5*	7.2
Glucose 6-phosphate	6.2*	7.6*	1.2	ND
Cysteine	2.6*	5.4*	2.1*	9.1

*Significant difference at $P \leq 0.05$. Values are shown for *cat2* SD and *cat2 pp2a-b′γ* SD (this study) and *cat2* LD (Chaouch *et al.*, 2012). All values are relative to the corresponding Col-0 values. ND, metabolite not detected in earlier study; + indicates metabolites induced in *cat2* in LD, but not detectable in Col-0; therefore, the fold change cannot be calculated.

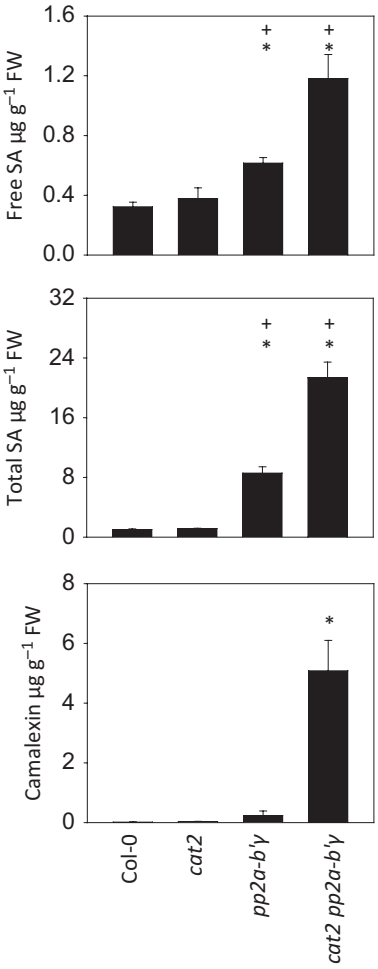

Fig. 5 Loss of PP2A-B′γ function allows the *cat2* mutation to trigger the accumulation of salicylic acid (SA) and camalexin in Arabidopsis growing in short days. Data are means ± SE of four biological replicates. * and +, significant difference relative to Col-0 or to *cat2* ($P < 0.05$). FW, fresh weight.

SA was observed in *pp2a-b′γ*, but the accumulation was much more marked in the double mutant, where total SA reached levels observed in *cat2* in LD (Fig. 1). Camalexin accumulation above basal Col-0 levels was only significant in *cat2 pp2a-b′γ*, in which levels of this compound were similar to those in *cat2* in LD (Fig 5; compare with Fig. 1). To establish whether the lesions associated with pathogenesis responses in *cat2 pp2a-b′γ* in SD were dependent on the SA pathway, triple mutants were produced that additionally carried either *sid2*, defective in SA synthesis (Wildermuth *et al.*, 2001), or *npr1*, defective in SA signaling (Cao *et al.*, 1994). In *cat2 pp2a-b′γ npr1*, lesions were significantly decreased, whereas, in *cat2 pp2a-b′γ sid2*, they were absent (Fig. 6). As reported previously for *cat2* growing in LD, lesion formation in *cat2 pp2a-b′γ* in SD could be prevented simply by treating plants with myo-inositol (Fig. 6), a compound that is implicated in the SA signaling pathway (Meng *et al.*, 2009; Chaouch & Noctor, 2010; Donahue *et al.*, 2010). Together, these results show that the lesions produced in *cat2 pp2a-b′γ* in SD were dependent on the SA pathway in a similar manner to the lesions observed in the *cat2* single mutant in LD.

Proteome and phosphoproteome modifications induced by the *pp2a-b′γ* mutation during oxidative stress

Next, we assessed how the features related to defense signaling were reflected in the proteome, and particularly the phosphoproteome, of *cat2 pp2a-b′γ* double mutant plants. First, we analyzed the pattern of phosphoproteins in total soluble and membrane fractions isolated from leaves of Col-0, *cat2*, *pp2a-b′γ* and *cat2 pp2a-b′γ* grown in SD. SDS-PAGE and subsequent quantitative ProQ staining of phosphoproteins, followed by Sypro staining of total proteins, showed no major changes between the *cat2* and *pp2a-b′γ* single mutants and Col-0 (Fig. S5). By contrast, a set of highly phosphorylated bands emerged in the

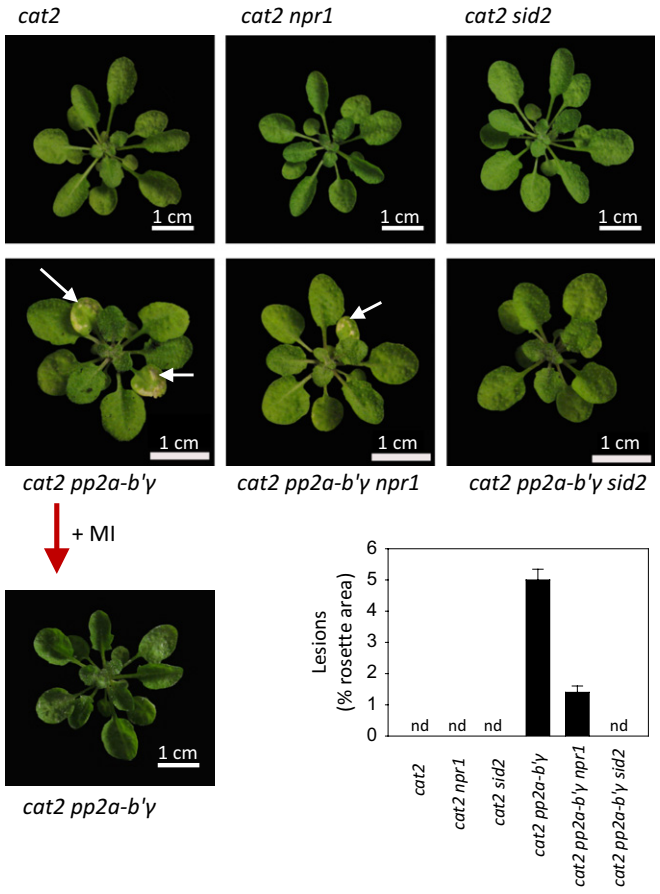

Fig. 6 Complete or partial genetic reversion of the Arabidopsis *cat2 pp2a-b′γ* lesion phenotype in short days by *sid2* and *npr1* mutations, and chemical blocking of the lesions by myo-inositol (MI) treatment. For lesion quantification, data are means ± SE (n = at least 10 plants). Examples of lesion-forming areas are indicated on the photographs by white arrows. nd, not detected.

soluble proteome of *cat2 pp2a-b′γ* double mutants (Fig. S5). None of the genotypes showed any major changes in the membrane fractions (Fig. S5).

Because neither single mutant showed marked changes in protein profiles, two-dimensional gel analysis was used to identify the phosphoproteins observed in *cat2 pp2a-b′γ*. This was performed in two successive steps. First, oligomeric protein complexes in total soluble leaf extracts were separated by CN-PAGE, followed by SDS-PAGE in the second dimension (Fig. 7), and stained with ProQ followed by Sypro. To detect the phosphopeptides, the gels were silver stained and the spots of interest were identified by MS and analysis of MS/MS spectra, allowing Ser, Thr and Tyr phosphorylation as possible modifications (Table 2; see Table S3 for technical details).

A number of spots with altered protein and/or phosphopeptide abundance between *cat2 pp2a-b′γ* and wild-type plants were observed (Fig. 7, Table 2). Proteins with different abundance included *S*-adenosyl-L-homocysteine hydrolase (SAHH) (spot 3, frame c), glutamine synthetase 1;1 (GLN1;1) and serine:glyoxylate aminotransferase (SGAT)/hydroxypyruvate reductase (spots 1 and 2, frame d), reflecting the marked changes observed in amino acid metabolism (Fig. S5), as well as copper/zinc superoxide dismutase (CSD2) and glutathione *S*-transferase PHI 2 (GSTF2) (spot 5 and 6, frame e), related to cellular redox homeostasis (Fig. 7, Table 2). These proteins have also been found previously to be affected in the *pp2a-b′γ* single mutant grown under different light and humidity conditions (130 µmol photons m^{-2} s^{-1}, 50% relative humidity; Trotta *et al.*, 2011a,b). The two-dimensional gel approach also identified a distinct spot containing AtMDAR2 (*Arabidopsis thaliana* monodehydroascorbate reductase2) (spot 3, frame d) in *cat2 pp2a-b′γ*, whereas, in the wild-type, this spot was barely visible (Fig. 7). In agreement with increased *PR1* transcripts (Fig. 2) and SA contents (Fig. 5), the double mutant also showed a marked accumulation of the SA-dependent proteins, PR2 and PR5 (spots 4 and 7, frame d). PR2 co-migrated with ACC oxidase 2 (ACO2), an ethylene-forming enzyme, which, like PR2, was not visible in Col-0 extracts (Fig. 7, Table 2).

With the exception of AtMDAR2, all the above-mentioned proteins contained phosphorylated peptides, and were thus identified as phosphoproteins (Table 2). Phosphopeptides specific for *cat2 pp2a-b′γ* were observed in SAHH and GSTF2, as well as in GLN1;1, PR2, PR5 and ACO2, proteins that were detectable only in the mutant extracts (Fig. 7, Table 2). SGAT, by contrast, contained two phosphopeptides that were detected in the wild-type, but not in *cat2 pp2a-b′γ* (Table 2).

Among the proteins recognized by ProQ, protein disulfide isomerase 2 (PDI2), Calreticulin 1 (CRT1) and CRT2 (spots 1, 5 and 6, respectively, frame c) showed a marked up-regulation of the protein level in *cat2 pp2a-b′γ* compared with wild-type plants (Fig. 7). MS revealed no phosphorylated residues in CRT1, whereas PDI1 and CRT2 contained phosphorylated peptides that were present in *cat2 pp2a-b′γ*, but not in the wild-type (Table 2). An increased phosphorylation level of elongation factor 1-α (EF1α) was also observed, indicative of regulatory changes at the level of protein synthesis in the cytosol as well (Fig. 7, Table 2).

The starch metabolism enzyme ADP glucose pyrophosphorylase large subunit 1 (AGPase) (spot 4, frame c) and an unknown protein At2g37660 (spot 5, frame d) were also detected by ProQ staining, but these proteins contained less phosphopeptides in *cat2 pp2a-b′γ* than in wild-type plants (Fig. 7, Table 2). In the intensively Sypro-stained spot 5 in frame (d), the protein with highest abundance was a chloroplastic 31-kDa RNA binding protein, but for which no phosphopeptides could be identified (Table 2). Spot 6 in frame (d) contained two phosphoproteins, HSP20-like protein and thiocyanate methyltransferase 1 (HOL1). Our previous study identified the myrosinase TGG1, a glucosinolate-degrading enzyme, as a distinctly up-regulated spot in *pp2a-b′γ* (Trotta *et al.*, 2011a), and this spot was evident in *cat2 pp2a-b′γ* (Fig. 7).

Two spots, containing a plastid isoform of triose phosphate isomerase (PDTPI) (spot 1, frame e) and carbonic anhydrase1 (CA1) (spot 3, frame e), appeared to be clearly down-regulated and contained less phosphopeptides in *cat2 pp2a-b′γ* relative to wild-type plants (Table 2). Although CA1 has been implicated in SA-dependent responses, the triose phosphate isomerase catalyzes

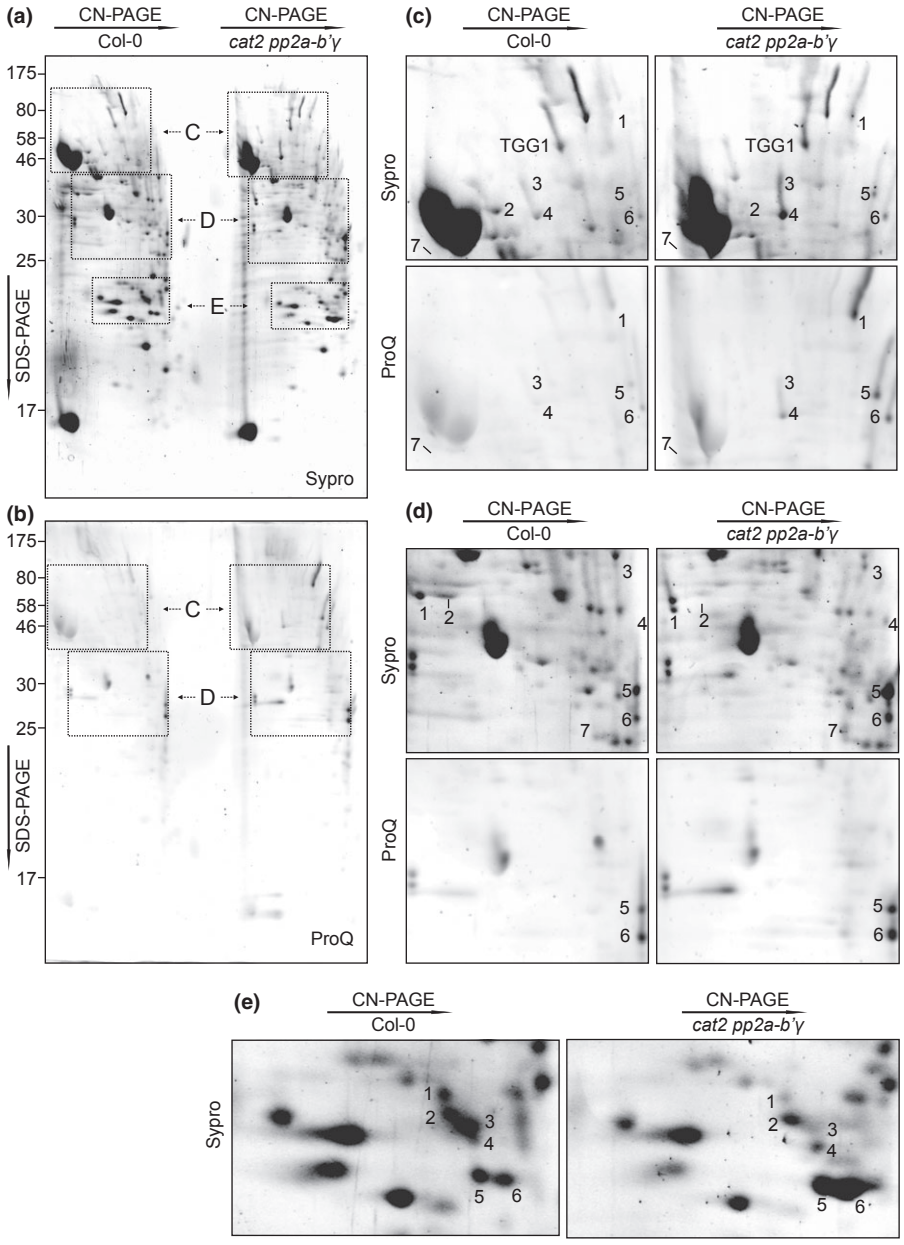

Fig. 7 Proteomic analysis of leaves of the Arabidopsis *cat2 pp2a-b′γ* double mutant growing in short days. (a, b) Representative Sypro-stained (a) and ProQ-stained (b) two-dimensional gels depicting proteins in the total foliar soluble fractions isolated from wild-type Col-0 and *cat2 pp2a-b′γ* plants. Oligomeric protein complexes were separated by clear-native polyacrylamide gel electrophoresis (CN-PAGE), followed by sodium dodecylsulfate (SDS)-PAGE in the second dimension. (c–e) Magnified frames from ProQ- and Sypro-stained gels showing areas with protein spots of higher or lower intensity in *cat2 pp2a-b′γ* relative to Col-0. The protein spots identified are indicated by sequential numbers in each frame, with each number indicating the same protein in *cat2 pp2a-b′γ* and Col-0. The proteins were identified by in-gel trypsin digestion and subsequent analysis by a nano-high-performance liquid chromatography-electrospray ionization-tandem mass spectrometry (nanoHPLC-ESI-MS/MS) system. Details concerning the identified proteins and phosphopeptides are presented in Table 2.

the conversion of glyceraldehyde 3-phosphate to dihydroxyacetone phosphate in the Benson–Calvin cycle.

Finally, we also found that CAT2 co-migrated as a high-molecular-weight oligomeric protein complex in the soluble leaf extract of wild-type plants, and also contained a phosphorylated Tyr residue at the C-terminal part of the protein (Fig. 7, spot 2, frame c). In *cat2 pp2a-b′γ*, the disappearance of CAT2 coincided with a decrease in the co-migrating SGAT (Fig. 7).

To determine whether the increased abundance detected at the protein level was accompanied by similar changes in transcript abundance, qPCR analysis of selected genes was performed. In agreement with the proteomics data (Table 2), *GLN1;1* and *GSTF2* transcripts were much more abundant in the double mutant than in other genotypes (Fig. 8a). This pattern was not observed for the transcripts of three other proteins found to accumulate in *cat2 pp2a-b′γ* (Fig. 8a), suggesting that their increased abundance could be related to regulation at the post-transcriptional level.

Flowering time and related gene expression in the different genotypes

Photoreceptors and regulation of flowering are among the possible pathways by which the *PP2A-B′γ*-dependent processes might mediate day length regulation of oxidative stress responses. This possibility was explored in two ways. First, an analysis was undertaken of the time taken to produce flowering stems in LD conditions, which promote the flowering program in Arabidopsis. No marked difference was observed between Col-0 and *cat2*, but the flowering stem appeared later in both the *pp2a-b′γ* single mutant

Table 2 Summary of proteins and phosphopeptides identified in soluble protein extracts of Arabidopsis leaves by two-dimensional clear-native polyacrylamide gel electrophoresis (CN-PAGE) and tandem mass spectrometry (MS/MS) analysis. Where corresponding phosphopeptides were detected, these are indicated in the right columns by 'X', and the peptide sequence containing the phosphorylated amino acid is given to the left.

Spot ID and change in *cat2 pp2a-b'γ*[a]	Full name	Gene	Phosphopeptides[b]	Col-0	*cat2 pp2a-b'γ*
Frame (c)					
1 ↑	Protein disulfide isomerase 2	At5g60640	VE(p)TTETKESPDSTTK		X
2 ↓	Catalase 2	At4g35090	LGPN(p)YLQLPVNAPK	X	
3 ↑	*S*-Adenosyl-L-homocysteine hydrolase 1	At4g13940	(p)TEFGPSQPFKGAR[c]	X	X
			(p)SKFDNLYGCR	X	X
	S-Adenosyl-L-homocysteine hydrolase 2	At3g23810	LVGV(p)SEETTTGVK	X	X
			GE(p)TLQEYWWCTER		X
4 ↑	ADP glucose pyrophosphorylase large subunit 1	At5g19220	V(P)YILTQYNSASLNR	X	
			(p)TVASIILGGGAGTR	X	X
5 ↑	Calreticulin-1	At1g56340			
6 ↑	Calreticulin-2	At1g09210	LL(p)SGDVDQKK		X
7 ↑	Elongation factor 1-α	At1g07940	G(p)YVASNSKDDPAK	X	X
			MTPTKPMVVE(p)TFSEYPPLGR	X	
			MTP(p)TKPMVVETFSEYPPLGR		X
			(p)STTTGHLIYK[d]	X	
			(p)YYCTVIDAPGHR		X
			VETGMIKPGMVV(p)TFAPTGLTTEVK		X
Frame (d)					
1 ↑	Glutamine synthetase 1;1	At5g37600	(p)TLPGPVTDPSQLPK		X
2 ↓	Serine:glyoxylate aminotransferase	At2g13360	L(p)SQDENHTIK	X	X
			(p)TLLEDVKK	X	X
			AL(p)SLPTGLGIVCASPK	X	
			AICIVHNE(p)TATGVTNDISAVR	X	
	Hydroxypyruvate reductase	At1g68010	EGMA(p)TLAALNVLGR	X	X
			A(p)SSMEEVLR	X	
3 ↑	Monodehydroascorbate reductase	At5g03630			
4 ↑	β-1,3-Glucanase2, pathogenesis-related protein 2	At3g57260	T(p)YVNNLIQHVK		X
			LA(p)SSQTEADKWVQENVQSYR[d]		X
			MRL(p)YGPDPGALAALR		X
	ACC oxidase 2	At1g62380	NASAVTELNPTAAVE(p)TF		X
			HLPQ(p)SNLNDISDVSDEYR		X
5 ↑	31-kDa RNA binding protein	At4g24770			
	3-β-Hydroxysteroid dehydrogenase domain-containing protein	At2g37660	ALF(p)TQVTTKF	X	
			(p)TGQIVYKK	X	X
6 ↑	HSP20-like	At4g02450	APAAEE(p)TTSVKEDK	X	X
	Thiocyanate methyltransferase 1	At2g43910	AV(p)SVEENPHAIPTR	X	X
			A(p)TPLIVHLVDTSSLPLGR		X
7 ↑	Pathogenesis-related gene 5	At1g75040	YAGCV(p)SDLNAACPDMLK		X
			NNCP(p)TTVWAGTLAGQGPK		X
Frame (e)					
1 ↓	Plastid isoform triose phosphate isomerase	At2g21170	EAGK(p)TFDVCFAQLK	X	X
			NV(p)SEEVASKTR	X	X
			VA(p)SPQQAQEVHVAVR	X	X
			GPEFA(p)TIVNSVTSKK	X	
2	Glutathione *S*-transferase TAU 20	At1g78370	FGNF(p)SIESESPK	X	X
			(p)SPLLLQSNPIHK	X	X
			(p)SLPDSEKIVAYAAEYR	X	
3↓	Carbonic anhydrase1	At3g01500	(p)YMVFACSDSR	X	
			(p)YETNPALYGELAK	X	
			YE(p)TNPALYGELAKGQSPK	X	X
			EK(p)YETNPALYGELAK	X	X
			EKYETNPAL(p)YGELAK	X	X
			EKYE(p)TNPALYGELAK		X
			G(p)TLALKGGYYDFVK	X	X
			VI(p)SELGDSAFEDQCGR	X	X
			VCP(p)SHVLDFQPGDAFVVR	X	X

Table 2 (Continued)

Spot ID and change in *cat2 pp2a-b′γ*[a]	Full name	Gene	Phosphopeptides[b]	Col-0	*cat2 pp2a-b′γ*
4	Glutathione *S*-transferase U19	At1g78380	GVEFEYREEDLR	X	X
			V(P)TEFVSELRK	X	X
			(p)SPLLLQMNPIHK	X	
5 ↑	Copper/zinc superoxide dismutase	At2g28190			
6 ↑	Glutathione *S*-transferase PHI 2	At4g02520	AI(p)TQYIAHR		X
			(p)SIYGLTTDEAVVAEEEAK		X
			(p)YENQGTNLLQTDSK		X

[a]The spot identifications are as presented in Fig. 7. Protein spots showing higher or lower intensity relative to the wild-type are indicated by upward or downward arrows, respectively.
[b]For the identification of phosphopeptides, Mascot analysis of MS/MS spectra was conducted by restricting searches for the Arabidopsis database and allowing the phosphorylation of threonine (Thr), serine (Ser) and tyrosine (Tyr) residues as possible modifications. Details on the identifications are presented in Table S3.
[c]This peptide is unique to At4g13940, whereas the others are identical for both isoforms.
[d]For these peptides, phosphoRS analysis was unable to indicate with high probability which residue is phosphorylated.

and *cat2 pp2a-b′γ* than in Col-0 and *cat2* (Fig. S6). Delayed flowering is in agreement with effects reported for the *pp2a-b′γ* mutant in a recent study of the role of PP2A subunits in flowering regulation (Heidari *et al.*, 2013). Second, the expression levels of three genes involved in the control of flowering (*CONSTANS* (*CO*), *FLOWERING LOCUS T* (*FLT*), *FLOWERING LOCUS C* (*FLC*)) were determined in SD, conditions in which the *pp2a-b′γ* mutant plays an important role in controlling the outcome of oxidative stress. This analysis revealed very low expression in all genotypes, and little or only slight differences between them (Fig. 8b). Slightly higher levels of *FLC* expression were observed in the *pp2a-b′γ* genotypes, although this was only significant for *cat2 pp2a-b′γ* (Fig. 8b). These increases were much less apparent than increases in FLC expression reported in *pp2a-b′γ* in LD (Heidari *et al.*, 2013). By contrast, clear differences were observed in phytochrome expression. In particular, *PHYTOCHROME A* (*PHYA*) transcripts were significantly less abundant in both *pp2a-b′γ* genotypes than in Col-0, with no difference between Col-0 and *cat2* (Fig. 8b).

Discussion

A previous report on the *pp2a-b′γ* single mutant provided the first evidence that PP2A-B′γ is an actor in the control of defense responses in Arabidopsis (Trotta *et al.*, 2011a). The present study provides new information on the role of this gene in determining day length-dependent responses to intracellular oxidative stress.

PP2A-B′γ is a key player in the negative control of day length-dependent SA-linked responses triggered by intracellular oxidative stress

Day length is emerging as an important control over responses of Arabidopsis to oxidative stress. In the *cat2* single mutant grown at moderate light, lesions and associated pathogenesis responses are observed in LD but not SD (Queval *et al.*, 2007; Chaouch *et al.*, 2010). The LD-dependent responses are absent in *cat2 sid2* and less apparent in *cat2 npr1* (Chaouch *et al.*, 2010; Han *et al.*, 2013a). LD conditions also promote lesion formation in mutants for other genes implicated in cell death pathways, such as *lesions simulating disease resistance1* (*lsd1*) and *myo-inositol phosphate synthase 1* (*mips1*) (Dietrich *et al.*, 1994; Meng *et al.*, 2009), although whether these responses are associated with intracellular oxidative stress remains unclear. The notion that day length context influences responses to oxidative stress (rather than just oxidative stress intensity) is supported by studies of plants exposed for equal times to ozone in different day length regimes (Vollsnes *et al.*, 2009; Dghim *et al.*, 2013).

The present data clearly establish *PP2A-B′γ* as a gene involved in the suppression of oxidative stress-driven lesions and related pathogenesis responses in SD. When introduced into the *cat2* background, the *pp2a-b′γ* mutation triggered hallmarks of the SA signaling pathway that were otherwise not observed. As well as lesion spread and SA itself, markers included the accumulation of camalexin and *PR1* transcripts. Activation of the pathway was also observed at the proteomic level. Although PR2 and PR5 phosphoproteins were not detected in the wild-type, both accumulated in the double mutant. Similar to *cat2* growing in LD, the activation of lesions in *cat2 pp2a-b′γ* is dependent on the isochorismate pathway of SA synthesis, as lesions were absent in the triple *cat2 pp2a-b′γ sid2* mutant.

Although the loss of *CAT2* function is not sufficient to activate pathogenesis responses in SD, some responses were observed in the *pp2a-b′γ* single mutant in this condition. These included some accumulation of SA, although camalexin and *PR1* expression remained at or close to wild-type levels. Although always less marked than in the double mutant, these responses in *pp2a-b′γ* were more pronounced in LD, conditions in which slight lesion formation was observed (Fig. 1), again underscoring the promotion of defense responses by long photoperiods. The activation of biotic stress defense responses in the *pp2a-b′γ* single mutant is in good agreement with the previous report of Trotta *et al.* (2011a),

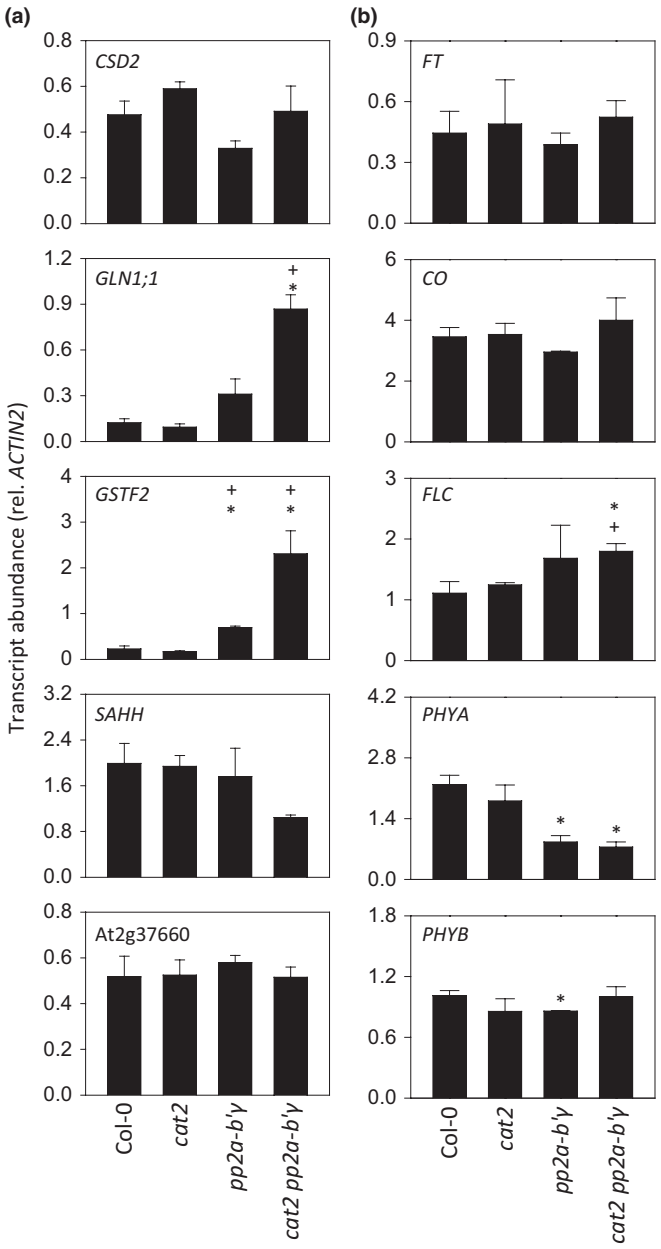

Fig. 8 Quantification of transcripts encoding differentially abundant proteins identified on the two-dimensional gels (a) and genes involved in flowering control or photoperiod signaling (b). Data are for Arabidopsis grown in short days. For explanation of abbreviations, see Supporting Information Table S1. Data are means ± SE of three biological replicates. For ease of expression, *FT* and *CO* values have been multiplied by 10 000, and *FLC* and *PHY* values by 100. Where significant, * and + indicate difference relative to Col-0 or to *cat2* ($P < 0.05$).

although some differences in the specific features of the responses were observed. Given the strong conditionality of plant responses to stress, differences could reflect the conditions used for the two studies. Phenotypes in the *pp2a-b′γ* single mutant are very sensitive to growth conditions, with lesions being less apparent as humidity or irradiance increases (A. Trotta & S. Kangasjärvi, unpublished). In the present study, both of these factors were higher than in that of Trotta *et al.* (2011a), possibly explaining why fewer lesions were observed in *pp2a-b′γ*. Despite their absence in both single mutants in SD in the growth conditions used in the present study, SA-dependent lesions were clearly apparent in *cat2 pp2a-b′γ*, underscoring the interaction between the two mutations.

A key role for PP2A-B′γ in regulating protein phosphorylation during oxidative stress

A number of phosphopeptides were differentially detectable when PP2A-B′γ function was lost in an oxidative stress context. Further studies will be required to establish whether these are substrates of PP2A oligomers containing this subunit, but three criteria can be used to identify the most interesting candidates: (1) the specificity for phosphoserine and phosphothreonine residues; (2) localization in the same compartments as PP2A-B′γ (cytosol, nucleus, plasmalemma; Table S4); and (3) increased phosphorylation status when PP2A-B′γ function is lost.

Based on these criteria, the best candidates to be direct targets during the oxidative stress response are SAHH, EF1α, HOL1, GSTF2, ACO2 and GLN1;1. The latter has previously been reported to be phosphorylated by calcium-dependent protein kinase (CDPK)-related kinase 3 (CRK3; Li *et al.*, 2006), and so its phosphorylation status may be influenced by the opposing actions of this kinase and PP2A-B′γ-dependent phosphatase activity. The roles of PP2A-B′γ may not be restricted to PP2A-dependent dephosphorylation, but could also involve inhibition of the activity of a cytosolic calcium-dependent kinase (CPK1) through physical interactions (G. Konert *et al.*, unpublished).

Whether or not these proteins are targets of PP2A-B′γ-dependent activities, our data provide clear evidence that this subunit is required to control the abundance or phosphorylation status of proteins during intracellular oxidative stress. Affected proteins include recognized players in redox homeostasis and associated signaling (HSP, GSTs, ACO2, CSD2, MDAR2, PR2, PR5). Indeed, GSTF2 has been described as a camalexin-binding protein (Dixon *et al.*, 2011), which is in accordance with the strong accumulation of this phytoalexin in *cat2 pp2a-b′γ* (Fig. 5). Further, PDI2, CRT1 and CRT2 all reside in the lumen of the endoplasmic reticulum (ER) and are connected to the unfolded protein response during ER stress that is implicated in pathogenesis responses (Trotta *et al.*, 2011b). Thus, PP2A-B′γ seems to be an integral part of the signaling hub that controls responses to oxidative stress at the proteomic level.

PP2A-B′γ as a central modulator of metabolic responses to oxidative stress

The *pp2a-b′γ* mutation not only allowed intracellular oxidative stress in SD to induce the accumulation of defense-related secondary metabolites, it also had a strong impact on the responses of primary metabolism. Intriguingly, SGAT was one of the proteins that showed opposite changes in abundance to the well-known SA-dependent PR2 and PR5 proteins (Table 2). This enzyme is one of at least two that act immediately downstream of

H_2O_2-producing glycolate oxidase to convert glyoxylate to glycine, and has been implicated previously in pathogenesis responses (Taler *et al.*, 2004). Our observations may suggest some co-regulation of the SGAT and CAT2 proteins. Although two independent microarray analyses show that *SGAT* transcripts are not significantly different in Col-0 and *cat2* (Mhamdi *et al.*, 2010c; Queval *et al.*, 2012), there is some evidence that peroxisomal enzymes involved in photorespiration can associate into complexes (Heupel *et al.*, 1991; Heupel & Heldt, 1994). The increased Ser in *cat2 pp2a-b′γ* may be a result of decreased SGAT abundance. Interestingly, however, Ser accumulation was less marked in the *cat2* single mutant (Fig. S4). As well as its stimulation by the *pp2a-b′γ* mutation, *cat2*-triggered Ser accumulation is largely blocked by the *sid2* mutation (Chaouch *et al.*, 2010). This suggests that any physical interaction may be conditional, possibly linked to SA signaling. If so, this could be relevant to the described roles of peroxisomal H_2O_2 and SGAT activity in pathogenesis responses (Taler *et al.*, 2004; Lipka *et al.*, 2005; Rojas *et al.*, 2012).

As well as Ser, many other amino acids are among the metabolites that are induced by *cat2* in LD in an SA-dependent manner (Chaouch *et al.*, 2010, 2012). Although much less or not accumulated in *cat2* in SD, several of these amino acids were strongly induced in the double mutant (Fig. 4; Table 1; Fig. S4). The accumulation of amino acids was correlated with the induction of GLN1;1, a cytosolic glutamine synthetase (GS1), at both protein and transcript levels (Table 2; Fig. 8). Similar to the accumulation of the GLN1;1 protein in *cat2 pp2a-b′γ*, GS1 protein was up-regulated in tomato plants infected with *Pseudomonas*, whereas the chloroplastic GS2 was down-regulated (Pérez-Garcia *et al.*, 1995). Opposing changes in the abundance of GS2 and GLN1;1 have also been observed previously in the *pp2a-b′γ* single mutant (Trotta *et al.*, 2011a). As GS2 is the photorespiratory isoform, it is linked to SGAT and CAT2 functions. By contrast, GS1 is associated with nitrogen remobilization, for example, during senescence (Pérez-Garcia *et al.*, 1995). One interpretation is that, in oxidative stress conditions, loss of PP2A-B′γ function down-regulates nitrogen cycling through the photorespiratory pathway in favor of the production of amino acids to support defense processes. This may occur to provide respiratory substrates for defense (Bolton, 2009), although other functions are possible. An amino acid transporter that may use glutamine as its major substrate has been implicated in the regulation of SA-dependent pathogenesis responses (Liu *et al.*, 2010).

Mutations leading to the loss of regulation of enzymes involved in the synthesis of the aspartate-derived amino acids trigger changes in resistance to specific pathogens (Stuttmann *et al.*, 2011). Alongside the activation of PR responses, isoleucine and Thr were both strongly accumulated in *cat2 pp2a-b′γ*, although two other aspartate-derived amino acids (homoserine and Met) were less affected. These last two compounds are involved in the Met cycle, a key source of methyl donors to various acceptors. Following methyl donation by *S*-adenosylmethionine (SAM), free homocysteine is regenerated by SAHH, proteins that were up-regulated in the double mutant (Table 2). Among many possible roles, methylation could be required for changes in secondary metabolism triggered by oxidative stress. Together with SAHH and PR proteins, *cat2 pp2a-b′γ* accumulated HOL1, which methylates the thiocyanate arising from the *in vivo* degradation of indolic glucosinolates (Nagatoshi & Nakamura, 2009). Methylation is also required in the synthesis of the coumarin, scopoletin, which accumulates in response to oxidative and biotic stress (Chong *et al.*, 2002; Fig. 1). As well as being used in methylation reactions, SAM can be withdrawn from the cycle and used for the synthesis of ethylene, with the first and limiting reaction catalyzed by ACC synthase (ACS). A study of the *roots curl in naphthylphthalamic acid1* (*rcn1*) mutant, which is deficient in a PP2A-A subunit, showed that two ACS isoforms were under differential control by PP2A-dependent processes (Skottke *et al.*, 2011), whereas we found significant up-regulation of ACO2 in *cat2 pp2a-b′γ*, allowing phosphorylation sites to be detected in this polypeptide. Thus, it seems likely that PP2A regulates both enzymatic steps required to convert SAM to ethylene.

Relationship of PP2A-B′γ function to intracellular oxidative stress

Growing evidence indicates that the outcome of oxidative stress is conditioned by other factors, and not simply related to oxidative stress intensity. The finding that the *pp2a-b′γ* mutation allows *cat2*-triggered pathogenesis responses to be produced in SD implicates PP2A-B′γ as an influential actor in responses to intracellular oxidative stress.

Key features of intracellular oxidative stress in *cat2* are the perturbation of intracellular thiol-disulfide status and the induction of a wide range of antioxidative genes (Mhamdi *et al.*, 2010c; Queval *et al.*, 2012), effects that are less evident in *pp2a-b′γ* (Fig. 3; Trotta *et al.*, 2011a). In contrast with *pp2a-b′γ* (Trotta *et al.*, 2011a) and *cat2 pp2a-b′γ* (this study), increases in DAB staining cannot be detected in *cat2* growing in our conditions. There are thus clear differences in the redox effects driven by the two mutations. Further, their association in the double mutant produces synergistic or qualitative effects on defense responses in SD, that is, their combination either produces a greater than additive effect (SA and camalexin contents) or triggers responses that are undetectable or close to negligible in the single mutants (lesions, *PR1* expression, several metabolites, proteomic profiles).

A key factor could be the interplay between ROS produced intracellularly and at the plasmalemma/apoplast. The activation of defense responses and the associated metabolic changes in *cat2* in LD are influenced by *AtRboh* function, pointing to interactions between oxidative stress inside the cell and ROS produced at the cell surface (Chaouch *et al.*, 2012). A primary role of PP2A-B′γ may be to restrict the activation of ROS production at the plasmalemma, explaining why the *pp2a-b′γ* mutant shows enhanced DAB staining (Trotta *et al.*, 2011a), which mainly detects extracellular ROS. The appearance of enhanced DAB staining in *cat2 pp2a-b′γ* may suggest that the loss of PP2A-B′γ function weakens the repression of extracellular ROS production. This could cause increased sensitivity to

cell-to-cell transmission of signals derived from perturbed intracellular redox status, triggering pathogenesis responses even in conditions in which they are not usually observed, and activating associated metabolic responses, such as nitrogen remobilization.

In conclusion, our study reveals that the repression of defense responses in SD is under genetic control through pathways linked to PP2A-B′γ function. Although further investigation is required to establish exactly how this is coupled to day length-dependent signaling, SA-dependent pathways are known to be modulated by photoreceptor functions (Genoud *et al.*, 2002; Martínez *et al.*, 2004; Griebel & Zeier, 2008). Decreased *PHYA* expression in the *pp2a-b′γ* genotypes (Fig. 8) suggests that photoreceptors may be involved in the regulatory nexus that links oxidative stress, day length, PP2A-B′γ and pathogenesis responses.

Acknowledgements

We thank the Salk Institute Genomic Analysis Laboratory (La Jolla, CA, USA) for providing the sequence-indexed Arabidopsis T-DNA insertion mutants and the Nottingham Arabidopsis Stock Centre (Nottingham, UK) for the supply of seed stocks. We are grateful to Patrick Saindrenan (IBP, Orsay, France) for the provision of HPLC facilities and the Turku Proteomics Facility (Turku, Finland) for excellent technical assistance. This work was supported by the European Union Initial Training Network 'COSI' and Academy of Finland projects 263772, 218157, 259888 and 130595.

References

Apel K, Hirt H. 2004. Reactive oxygen species: metabolism, oxidative stress, and signal transduction. *Annual Review of Plant Biology* **55**: 373–399.

Ball L, Accotto G, Bechtold U, Creissen G, Funck D, Jimenez A, Kular B, Leyland N, Mejia-Carranza J, Reynolds H *et al.* 2004. Evidence for a direct link between glutathione biosynthesis and stress defense gene expression in Arabidopsis. *Plant Cell* **16**: 2448–2462.

Bechtold U, Karpinski S, Mullineaux PM. 2005. The influence of the light environment and photosynthesis on oxidative signalling responses in plant–biotrophic pathogen interactions. *Plant, Cell & Environment* **28**: 1046–1055.

Becker B, Holtgrefe S, Jung S, Wunrau C, Kandlbinder A, Baier M, Dietz K-J, Backhausen JE, Scheibe R. 2006. Influence of the photoperiod on redox regulation and stress responses in *Arabidopsis thaliana* L. (Heynh.) plants under long and short-day conditions. *Planta* **224**: 380–393.

Bolton MD. 2009. Primary metabolism and plant defense – fuel for the fire. *Molecular Plant–Microbe Interactions* **22**: 487–497.

Cao H, Bowling SA, Gordon AS, Dong X. 1994. Characterization of an Arabidopsis mutant that is nonresponsive to inducers of systemic acquired resistance. *Plant Cell* **6**: 1583–1592.

Chaouch S, Noctor G. 2010. *Myo*-inositol abolishes salicylic acid-dependent cell death and pathogen defence responses triggered by peroxisomal H_2O_2. *New Phytologist* **188**: 711–718.

Chaouch S, Queval G, Noctor G. 2012. AtRbohF is a crucial modulator of defence-associated metabolism and a key actor in the interplay between intracellular oxidative stress and pathogenesis responses in Arabidopsis. *Plant Journal* **69**: 613–627.

Chaouch S, Queval G, Vanderauwera S, Mhamdi A, Vandorpe M, Langlois-Meurinne M, Van Breusegem F, Saindrenan P, Noctor G. 2010. Peroxisomal hydrogen peroxide is coupled to biotic defense responses by ISOCHORISMATE SYNTHASE1 in a daylength-related manner. *Plant Physiology* **153**: 1692–1705.

Chong J, Baltz R, Schmitt C, Beffa R, Fritig B, Saindrenan P. 2002. Downregulation of a pathogen–responsive tobacco UDP–Glc:phenylpropanoid glucosyltransferase reduces scopoletin glucoside accumulation, enhances oxidative stress, and weakens virus resistance. *Plant Cell* **14**: 1093–1107.

Dghim AA, Mhamdi A, Vaultier MV, Hasenfratz-Sauder MP, Le Thiec D, Dizengremel P, Noctor G, Jolivet E. 2013. Analysis of cytosolic isocitrate dehydrogenase and glutathione reductase 1 in photoperiod-influenced responses to ozone using Arabidopsis knockout mutants. *Plant, Cell & Environment* **36**: 1981–1991.

Dietrich RA, Delaney TP, Uknes SJ, Ward ER, Ryals JA, Dangl JL. 1994. Arabidopsis mutants simulating disease resistance response. *Cell* **7**: 565–572.

Dixon DP, Sellars JD, Edwards R. 2011. The Arabidopsis phi class glutathione transferase AtGSTF2: binding and regulation by biologically active heterocyclic ligands. *Biochemical Journal* **438**: 63–70.

Donahue JL, Alford SR, Torabinejad J, Kerwin RE, Nourbakhsh A, Ray WK, Hernick M, Huang X, Lyons BM, Hein PP *et al.* 2010. The *Arabidopsis thaliana Myo*-inositol 1-phosphate synthase1 gene is required for *Myo*-inositol synthesis and suppression of cell death. *Plant Cell* **22**: 888–903.

Foyer CH, Noctor G. 2009. Redox regulation in photosynthetic organisms: signaling, acclimation, and practical implications. *Antioxidants & Redox Signaling* **11**: 861–905.

Genoud T, Buchala AJ, Chua N-H, Métraux J-P. 2002. Phytochrome signalling modulates the SA-perceptive pathway in *Arabidopsis*. *Plant Journal* **31**: 87–95.

Glawischnig E. 2007. Camalexin. *Phytochemistry* **68**: 401–406.

Griebel T, Zeier J. 2008. Light regulation and daytime dependency of inducible plant defenses in Arabidopsis: phytochrome signaling controls systemic acquired resistance rather than local defense. *Plant Physiology* **147**: 790–801.

Han Y, Chaouch S, Mhamdi A, Queval G, Zechmann B, Noctor G. 2013a. Functional analysis of Arabidopsis mutants points to novel roles for glutathione in coupling H_2O_2 to activation of salicylic acid accumulation and signaling. *Antioxidants & Redox Signaling* **18**: 2087–2090.

Han Y, Mhamdi A, Chaouch S, Noctor G. 2013b. Regulation of basal and oxidative stress-triggered jasmonic acid-related gene expression by glutathione. *Plant, Cell & Environment* **36**: 1135–1146.

Heidari B, Nemie-Feyissa D, Kangasjärvi S, Lillo C. 2013. Antagonistic regulation of flowering time through distinct regulatory subunits of protein phosphatase 2A. *PLoS One* **8**: e67987.

Heupel R, Heldt HW. 1994. Protein organization in the matrix of leaf peroxisomes. A multi-enzyme complex involved in photorespiratory metabolism. *European Journal of Biochemistry* **220**: 165–172.

Heupel R, Markgraf T, Robinson DG, Heldt HW. 1991. Compartmentation studies on spinach leaf peroxisomes. Evidence for channeling of photorespiratory metabolites in peroxisomes devoid of intact boundary membranes. *Plant Physiology* **96**: 971–979.

Kangasjärvi S, Lepistö A, Hännikäinen K, Piippo M, Luomala EM, Aro EM, Rintamäki E. 2008. Diverse roles for chloroplast stromal and thylakoid-bound ascorbate peroxidases in plant stress responses. *Biochemical Journal* **412**: 275–285.

Kangasjärvi S, Neukermans J, Li S, Aro EM, Noctor G. 2012. Photosynthesis, photorespiration, and light signalling in defence responses. *Journal of Experimental Botany* **63**: 1619–1636.

Kovtun Y, Chiu WL, Tena G, Sheen J. 2000. Functional analysis of oxidative stress-activated mitogen-activated protein kinase cascade in plants. *Proceedings of the National Academy of Sciences, USA* **97**: 2940–2945.

Langlois-Meurinne M, Gachon CMM, Saindrenan P. 2005. Pathogen-responsive expression of glycosyltransferase genes *UGT73B3* and *UGT73B5* is necessary for resistance to *Pseudomonas syringae* pv *tomato* in Arabidopsis. *Plant Physiology* **139**: 1890–1901.

Li J, Hua W, Lu Y. 2006. Arabidopsis cytosolic glutamine synthetase AtGLN1;1 is a potential substrate of AtCRK3 involved in leaf senescence. *Biochemical and Biophysical Research Communication* **342**: 119–126.

Lipka V, Dittgen J, Bednarek P, Bhat R, Wiermer M, Stein M, Landtag J, Brandt W, Rosahl S, Scheel D *et al.* 2005. Pre- and post-invasion defenses

both contribute to non-host resistance in Arabidopsis. *Science* **310**: 1180–1183.

Liu G, Ji Y, Bhuiyan NH, Pilot G, Salvaraj G, Zou J, Wei Y. 2010. Amino acid homeostasis modulates salicylic acid-associated redox status and defense responses in *Arabidopsis*. *Plant Cell* **22**: 3845–3863.

MacKintosh C, Cohen P. 1989. Identification of high levels of type 1 and type 2A protein phosphatases in higher plants. *Biochemical Journal* **262**: 335–339.

Martínez C, Pons E, Prats G, León J. 2004. Salicylic acid regulates flowering time and links defence responses and reproductive development. *Plant Journal* **37**: 209–217.

Meng PH, Raynaud C, Tcherkez G, Blanchet S, Massoud K, Domenichini S, Henry Y, Soubigou-Taconnat L, Lelarge-Trouverie C, Saindrenan P *et al.* 2009. Crosstalks between myo-inositol metabolism, programmed cell death and basal immunity in *Arabidopsis*. *PLoS One* **4**: e7364.

Mhamdi A, Hager J, Chaouch S, Queval G, Han Y, Taconnat Y, Saindrenan P, Issakidis-Bourguet E, Gouia H, Renou JP *et al.* 2010c. *Arabidopsis* GLUTATHIONE REDUCTASE 1 is essential for the metabolism of intracellular H_2O_2 and to enable appropriate gene expression through both salicylic acid and jasmonic acid signaling pathways. *Plant Physiology* **153**: 1144–1160.

Mhamdi A, Mauve C, Gouia H, Saindrenan P, Hodges M, Noctor G. 2010b. Cytosolic NADP-dependent isocitrate dehydrogenase contributes to redox homeostasis and the regulation of pathogen responses in *Arabidopsis* leaves. *Plant, Cell & Environment* **33**: 1112–1123.

Mhamdi A, Queval G, Chaouch S, Vanderauwera S, Van Breusegem F, Noctor G. 2010a. Catalase in plants: a focus on Arabidopsis mutants as stress-mimic models. *Journal of Experimental Botany* **61**: 4197–4220.

Michelet L, Krieger-Liszkay A. 2011. Reactive oxygen intermediates produced by photosynthetic electron transport are enhanced in short-day grown plants. *Biochimica et Biophysica Acta* **1817**: 1306–1313.

Nagatoshi Y, Nakamura T. 2009. *Arabidopsis* HARMLESS TO OZONE LAYER protein methylates a glucosinolate breakdown product and functions in resistance to *Pseudomonas syringae* pv. *maculicola*. *Journal of Biological Chemistry* **284**: 19301–19309.

Noctor G, Bergot G, Mauve C, Thominet D, Lelarge-Trouverie C, Prioul J-L. 2007. A comparative study of amino acid measurement in leaf extracts by gas chromatography–time of flight–mass spectrometry and high performance liquid chromatography with fluorescence detection. *Metabolomics* **3**: 161–174.

Noctor G, Hager J, Li S. 2011. Biosynthesis of NAD and its manipulation in plants. *Advances in Botanical Research* **58**: 153–201.

Overmyer K, Brosché M, Kangasjärvi J. 2003. Reactive oxygen species and hormonal control of cell death. *Trends in Plant Science* **8**: 335–342.

Parisy V, Poinssot B, Owsianowski L, Buchala A, Glazebrook J, Mauch F. 2007. Identification of PAD2 as a γ-glutamylcysteine synthetase highlights the importance of glutathione in disease resistance in Arabidopsis. *Plant Journal* **49**: 159–172.

Pastori GM, Kiddle G, Antoniw J, Bernard S, Veljovic-Jovanovic S, Verrier PJ, Noctor G, Foyer CH. 2003. Leaf vitamin C contents modulate plant defense transcripts and regulate genes that control development through hormone signaling. *Plant Cell* **15**: 939–951.

Peltier JB, Cai Y, Sun Q, Zabrouskov V, Giacomelli L, Rudella A, Ytterberg AJ, Rutschow H, van Wijk KJ. 2006. The oligomeric stromal proteome of *Arabidopsis thaliana* chloroplasts. *Molecular & Cellular Proteomics* **5**: 114–133.

Pérez-Garcia A, Canovas FM, Gallardo F, Hirel B, De Vicente A. 1995. Differential expression of glutamine synthetase isoforms in tomato detached leaflets infected with *Pseudomonas syringae* pv. *tomato*. *Molecular Plant–Microbe Interactions* **8**: 96–103.

Pérez-Pérez JM, Esteve-Bruna D, González-Bayóna R, Kangasjärvi S, Caldana C, Hannah MA, Willmitzer L, Poncea MR, Micola JL. 2013. Functional redundancy and divergence within the Arabidopsis RETICULATA-RELATED gene family. *Plant Physiology* **162**: 589–603.

Queval G, Hager J, Gakière B, Noctor G. 2008. Why are literature data for H_2O_2 contents so variable? A discussion of potential difficulties in quantitative assays of leaf extracts. *Journal of Experimental Botany* **59**: 135–146.

Queval G, Issakidis-Bourguet E, Hoeberichts FA, Vandorpe M, Gakière B, Vanacker H, Miginiac-Maslow M, Van Breusegem F, Noctor G. 2007. Conditional oxidative stress responses in the Arabidopsis photorespiratory mutant *cat2* demonstrate that redox state is a key modulator of daylength-dependent gene expression, and define photoperiod as a crucial factor in the regulation of H_2O_2-induced cell death. *Plant Journal* **52**: 640–657.

Queval G, Neukermans J, Vanderauwera S, Van Breusegem F, Noctor G. 2012. Day length is a key regulator of transcriptomic responses to both CO_2 and H_2O_2 in Arabidopsis. *Plant, Cell & Environment* **35**: 374–387.

Queval G, Noctor G. 2007. A plate reader method for the measurement of NAD, NADP, glutathione, and ascorbate in tissue extracts: application to redox profiling during Arabidopsis rosette development. *Analytical Biochemistry* **363**: 58–69.

Queval G, Thominet D, Vanacker H, Miginiac-Maslow M, Gakière B, Noctor G. 2009. H_2O_2-activated up-regulation of glutathione in Arabidopsis involves induction of genes encoding enzymes involved in cysteine synthesis in the chloroplast. *Molecular Plant* **2**: 344–356.

Rojas CM, Senthil-Kumar M, Wang K, Ryu CM, Kaundal A, Mysore KS. 2012. Glycolate oxidase modulates reactive oxygen species-mediated signal transduction during nonhost resistance in *Nicotiana benthamiana* and Arabidopsis. *Plant Cell* **24**: 336–352.

Rokka A, Suorsa M, Saleem A, Battchikova N, Aro EM. 2005. Synthesis and assembly of thylakoid protein complexes: multiple assembly steps of photosystem II. *Biochemical Journal* **388**: 159–168.

Skottke KR, Yoon GM, Kieber JJ, DeLong A. 2011. Protein phosphatase 2A controls ethylene biosynthesis by differentially regulating the turnover of ACC synthase isoforms. *PLoS Genetics* **7**: e1001370.

Smith IK, Kendall AC, Keys AJ, Turner JC, Lea PJ. 1984. Increased levels of glutathione in a catalase-deficient mutant of barley (*Hordeum vulgare* L.). *Plant Science Letters* **37**: 29–33.

Stuttmann J, Hubberten H-M, Rietz S, Kaur J, Muskett P, Guerois R, Bednarek P, Hoefgen R, Parker JE. 2011. Perturbation of Arabidopsis amino acid metabolism causes incompatibility with the adapted biotrophic pathogen *Hyaloperonospora arabidopsidis*. *Plant Cell* **23**: 2788–2803.

Taler D, Galperin M, Benjamin I, Cohen Y, Kenigsbuch D. 2004. Plant *eR* genes that encode photorespiratory enzymes confer resistance against disease. *Plant Cell* **16**: 172–184.

Trotta A, Konert G, Rahikainen M, Aro EM, Kangasjärvi S. 2011b. Knock-down of protein phosphatase 2A subunit B′γ promotes phosphorylation of CALRETICULIN 1 in *Arabidopsis thaliana*. *Plant Signal Behavior* **6**: 1665–1668.

Trotta A, Wrzaczek M, Scharte J, Tikkanen M, Konert G, Rahikainen M, Holmström M, Hiltunen HM, Rips S, Sipari N *et al.* 2011a. Regulatory subunit B′gamma of protein phosphatase 2A prevents unnecessary defense reactions under low light in Arabidopsis. *Plant Physiology* **156**: 1464–1480.

Van Breusegem F, Bailey-Serres J, Mittler R. 2008. Unraveling the tapestry of networks involving reactive oxygen species in plants. *Plant Physiology* **147**: 978–984.

Vollsnes AV, Erikson AB, Otterholt E, Kvaal K, Oxaal U, Futsaether C. 2009. Visible foliar injury and infrared imaging show that daylength affects short-term recovery after ozone stress in *Trifolium subterraneum*. *Journal of Experimental Botany* **60**: 3677–3686.

Wagner D, Przybyla D, Op den Camp R, Kim C, Landgraf F, Lee KP, Würsch M, Laloi C, Nater M, Hideg E *et al.* 2004. The genetic basis of singlet oxygen-induced stress responses of *Arabidopsis thaliana*. *Science* **306**: 1183–1185.

Wildermuth MC, Dewdney J, Wu G, Ausubel FM. 2001. Isochorismate synthase is required to synthesize salicylic acid for plant defence. *Nature* **414**: 562–565 [Err Nature 417: 571].

Willekens H, Chamnongpol S, Davey M, Schraudner M, Langebartels C, Van Montagu M, Inzé D, Van Camp W. 1997. Catalase is a sink for H_2O_2 and is indispensable for stress defence in C_3 plants. *EMBO Journal* **16**: 4806–4816.

Zhou HW, Nussbaumer C, Chao Y, DeLong A. 2004. Disparate roles for the regulatory A subunit isoforms in Arabidopsis protein phosphatase 2A. *Plant Cell* **16**: 709–722.

Supporting Information

Additional supporting information may be found in the online version of this article.

Fig. S1 Production and genotyping of mutant lines.

Fig. S2 Ascorbate and glutathione contents in plants grown in long days (LD).

Fig. S3 Phenotypes and glutathione contents in mutants grown at low light.

Fig. S4 Amino acid contents in the *cat2 pp2a-b′γ* double mutant.

Fig. S5 Pattern of phosphoproteins in total soluble and membrane fractions isolated from wild-type, *cat2*, *pp2a-b′γ* and *cat2 pp2a-b′γ* leaves.

Fig. S6 Analysis of flowering time in Col-0 and mutant lines.

Table S1 Primer sequences used in this study

Table S2 Full list of metabolites detected by gas chromatography-time of flight-mass spectrometry (GC-TOF-MS)

Table S3 Ion scores, masses observed and expectation values for the identified phosphopeptides presented in Table 2

Table S4 Likely subcellular localization of proteins modified in abundance or phosphorylation status in *cat2 pp2-a-b′γ*

Please note: Wiley Blackwell are not responsible for the content or functionality of any supporting information supplied by the authors. Any queries (other than missing material) should be directed to the *New Phytologist* Central Office